Mineralogical Magazine, April 2013, Vol. 77(3), pp. 385–398

Hylbrownite, $Na_3MgP_3O_{10}\cdot 12H_2O$, a new triphosphate mineral from the Dome Rock Mine, South Australia: description and crystal structure

P. Elliott[1,2]*, J. Brugger[1,2], T. Caradoc-Davies[3] and A. Pring[2]

[1] School of Earth and Environmental Sciences, The University of Adelaide, Adelaide, South Australia 5005, Australia
[2] South Australian Museum, North Terrace, Adelaide, South Australia 5000, Australia
[3] Australian Synchrotron, 800 Blackburn Road, Clayton, Victoria 3168, Australia

[*Received 10 December 2012; Accepted 8 April 2013; Associate Editor: Wilson Crichton*]

ABSTRACT

Hylbrownite, ideally $Na_3MgP_3O_{10}\cdot 12H_2O$, the second known triphosphate mineral, is a new mineral species from the Dome Rock mine, Boolcoomatta Reserve, Olary Province, South Australia, Australia. The mineral forms aggregates and sprays of crystals up to 0.5 mm across with individual crystals up to 0.12 mm in length and 0.02 mm in width. Crystals are thin prismatic to acicular in habit and are elongate along [001]. Forms observed are {010}, {100}, {001}, {210} and {201}. Crystals are colourless to white, possess a white streak, are transparent, brittle, have a vitreous lustre and are non-fluorescent. The measured density is 1.81(4) g cm^{-3}; Mohs' hardness was not determined. Cleavage is good parallel to {001} and to {100} and the fracture is uneven. Hylbrownite crystals are nonpleochroic, biaxial (−), with α = 1.390(4), β = 1.421(4), γ = 1.446(4) and $2V_{calc.}$ = 82.2°. Hylbrownite is monoclinic, space group $P2_1/n$, with a = 14.722(3), b = 9.240(2), c = 15.052(3) Å, β = 90.01(3)°, V = 2047.5(7) Å^3, (single-crystal data) and Z = 4. The strongest lines in the powder X-ray diffraction pattern are [d(Å)(I)(hkl)]: 10.530(60)(10$\bar{1}$,101), 7.357(80)(200), 6.951(100)(11$\bar{1}$, 111), 4.754(35)(10$\bar{3}$, 103), 3.934(40)(022), 3.510(45)(30$\bar{3}$, 303), 3.336(35)(41$\bar{1}$, 411). Chemical analysis by electron microprobe gave Na_2O 16.08, MgO 7.08, CaO 0.43, P_2O_5 37.60, H_2O_{calc} 38.45, total 99.64 wt.%. The empirical formula, calculated on the basis of 22 oxygen atoms is $Na_{2.93}Mg_{0.99}Ca_{0.04}P_{2.99}O_{9.97}\cdot 12.03H_2O$. The crystal structure was solved from single-crystal X-ray diffraction data using synchrotron radiation (T = 123 K) and refined to R_1 = 4.50% on the basis of 2417 observed reflections with $F_0 > 4\sigma(F_0)$. $[Mg(H_2O)_3P_3O_{10}]$ clusters link in the b direction to $Na\phi_6$ octahedra, by face and corner sharing. Edge sharing $Na\phi_6$ octahedra and $Na\phi_7$ polyhedra form Na_2O_9 groups which link via corners to form chains along the b direction. Chains link to $[Mg(H_2O)_3P_3O_{10}]$ clusters via corner-sharing in the c direction and form a thick sheet parallel to (100). Sheets are linked in the a direction via hydrogen bonds.

Keywords: hylbrownite, new mineral species, triphosphate, crystal structure, Dome Rock mine.

Introduction

Hylbrownite occurs on two specimens collected from the Dome Rock mine, which is situated on Boolcoomatta Reserve, a former sheep station that is now a Bush Heritage reserve, 42 km north of the railway siding of Mingary and ~470 km northeast of Adelaide, South Australia. It is not known when the specimens were collected; probably during the 1980s when the mine was being worked for mineral specimens. The Dome

* E-mail: peter.elliott@adelaide.edu.au
DOI: 10.1180/minmag.2013.077.3.11

Rock mine is well known for a suite of secondary arsenate minerals, including agardite, arseniosiderite, clinoclase, erythrite, lavendulan, metazeunerite, olivenite, scorodite and smolianinovite (Bayliss *et al.*, 1966; Kleeman and Milnes, 1973; Ryall and Segnit, 1976; Segnit, 1978). It is the type locality for cobaltaustinite (Nickel and Birch, 1988) and the new mineral domerockite (IMA2009-016). One secondary phosphate mineral has previously been recorded, fluorapatite, which occurs as colourless, tabular to short prismatic microcrystals that are commonly seen scattered on earlier formed arsenates (Ryall and Segnit, 1976).

The new species is named for Henry Yorke Lyell Brown (1844–1928), Government Geologist of South Australia from 1882 to 1912. Brown made the first recorded observations of much of the interior of the state of South Australia and the Northern Territory and produced the first geological map of the whole colony in 1899. He documented the mineral resources of South Australia and published numerous reports, four editions of *The Records of the Mines of South Australia* (Brown, 1908) and also the *Catalogue of South Australian Minerals* (Brown, 1893).

Hylbrownite has a synthetic analogue (Rakotomahanina *et al*., 1972). The new mineral and mineral name have been approved by the IMA Commission on New Minerals, Nomenclature and Classification (IMA 2010-054). The holotype specimen is preserved in the collection of the South Australian Museum, Adelaide, South Australia, (Registration number G33088).

Occurrence

The Dome Rock deposit comprises several small, independent, lenticular orebodies at shallow depth, situated in Lower Proterozoic metasediments of the Willyama Complex on the northern flank of an E−W striking range which is composed mostly of granitic rocks (Dickinson, 1942). The ore-bodies are interpreted as being hypergene in origin and most likely related to the invasion of metasediments by granite intrusives. Mineralizing solutions gained access to the sediments along channels formed either by minor faults or along favourable rock contacts.

The suite of secondary arsenate minerals formed by oxidation of primary sulphides, principally chalcopyrite, chalcocite, arsenopyrite and cobaltite, under low-temperature conditions. The secondary phosphates hylbrownite and fluorapatite formed later than the arsenate minerals. No primary P minerals have been recorded from the Dome Rock mine, however, a number of P-bearing pegmatites are located nearby and these may have been the source of P for the phosphate minerals.

The synthetic analogue of hylbrownite was prepared at room temperature by titration of sodium triphosphate with a solution of an Mg salt (Rakotomahanina *et al.*, 1972) so natural samples almost certainly crystallized at ambient (~25ºC) temperatures.

On the holotype specimen, hylbrownite occurs in a thin seam as aggregates and sprays of crystals, overgrowing aggregates of pale green conichalcite, crusts of chrysocolla and crusts of a black, amorphous Cu-Mn-Co silicate. The matrix comprises grey quartzite with very minor goethite and muscovite. On a second specimen, hylbrownite crystal sprays occur on an iron oxide-stained quartzite matrix associated with cuprite, malachite, azurite and goethite.

Appearance, physical and optical properties

Hylbrownite occurs as aggregates and sprays of crystals to 0.5 mm across with individual crystals up to 0.12 mm in length and 0.02 mm in width (Fig. 1). Crystals are thin prismatic to acicular in habit, elongate along [001]. Forms observed are {010}, {100}, {001}, {210} and {201}. The mineral is colourless to white, the streak is white, and the lustre is vitreous. Mohs' hardness was not determined due to the small size of the crystals. The density, measured by the sink-float method in an aqueous solution of sodium polytungstate is

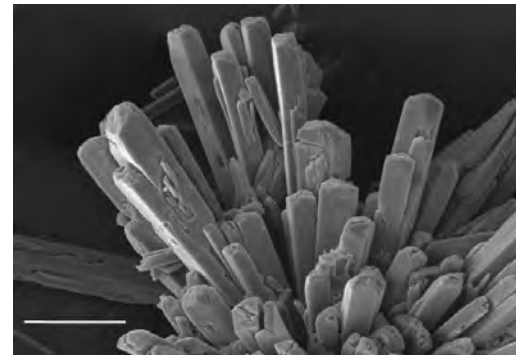

FIG. 1. SEM photomicrograph showing acicular crystals of hylbrownite. The scale bar is 50 μm long.

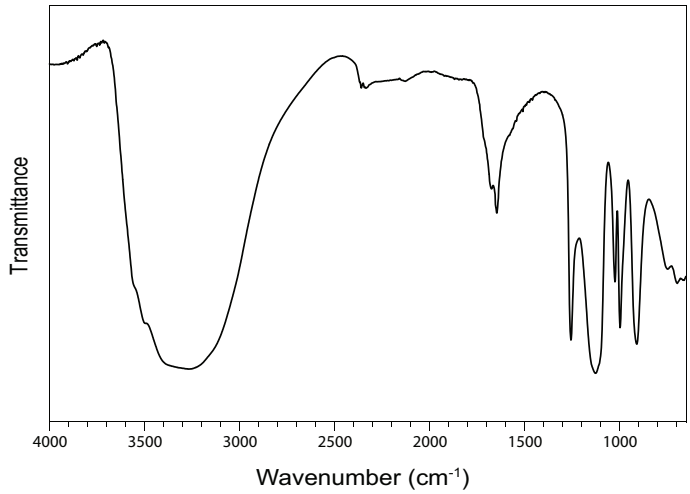

FIG. 2. FTIR spectrum of powdered hylbrownite.

1.81(4) g cm^{-3}, whilst the calculated density from the empirical formula is 1.82 g cm^{-3}. Tenacity is brittle. Cleavage is good parallel to {001} and to {100} and the fracture is uneven. The mineral is nonpleochroic, biaxial (−), with $\alpha = 1.390(4)$, $\beta = 1.421(4)$, $\gamma = 1.446(4)$ and $2V_{calc.} = 82.2°$. The Gladstone-Dale compatibility index (Mandarino, 1981) is 0.066, categorized as fair.

Chemical composition

Crystals of hylbrownite were analysed using a Cameca SX-51 electron microprobe operating in wavelength dispersion mode, with an accelerating voltage of 15 kV, a specimen current of 10 nA, and a beam diameter of 20 μm. An energy-dispersive scan indicated the absence of any other elements with atomic number greater than 8, in quantities greater than 0.05 wt.%. The data were reduced and corrected by the 'PAP' method of Pouchou and Pichoir (1985). The presence of H_2O groups was established by crystal-structure solution and infrared-absorption spectroscopy. A good polish for the electron microprobe work could not be obtained, and this coupled with extreme instability under the electron beam resulted in analytical results that are very variable. The mean analytical results are reported in Table 1; the empirical formula based on 22 oxygen atoms is $Na_{2.93}Mg_{0.99}Ca_{0.04}P_{2.99}O_{9.97} \cdot 12.03H_2O$. The simplified formula is $Na_3MgP_3O_{10} \cdot 12H_2O$, which requires (in wt.%) Na_2O 16.53, MgO 7.17, P_2O_5 37.86, H_2O 38.45, total 100.00 wt.%.

TABLE 1. Compositional data for hylbrownite.

Constituent	Wt.%	Range	Stand. Dev.	Probe Standard
Na_2O	16.08	15.11−17.15	0.70	albite
MgO	7.08	5.56−8.94	1.17	almandine
CaO	0.43	0.18−0.63	0.16	hydroxylapatite
P_2O_5	37.60	35.7−40.28	1.67	hydroxylapatite
H_2O*	38.45			
Total	99.64			

Number of analyses = 9.
* calculated from the ideal formula based on structure determination.

TABLE 2. X-ray powder diffraction data for hylbrownite.

I_{obs}	d_{obs}	I_{calc}	d_{calc}	h	k	l	I_{obs}	d_{obs}	I_{calc}	d_{calc}	h	k	l
60	10.530	74	10.526	1	0	$\bar{1}$	10	2.860	8	2.862	1	$\bar{2}$	$\bar{4}$
		57	10.524	1	0	1	15	2.855	21	2.851	0	3	2
20	7.869	16	7.875	0	1	1			16	2.828	4	2	$\bar{1}$
		10	7.526	0	0	2	25	2.831	13	2.826	4	$\bar{1}$	$\bar{3}$
80	7.357	100	7.361	2	0	0			7	2.825	4	1	3
100	6.949	95	6.944	1	1	$\bar{1}$	5	2.691	8	2.689	4	2	2
		40	6.944	1	1	1			6	2.668	2	$\bar{1}$	$\bar{5}$
30	5.835	41	5.835	0	1	2	5	2.669	7	2.668	2	1	5
		5	5.425	1	$\bar{1}$	$\bar{2}$	10	2.627	13	2.625	0	3	3
		6	5.377	2	1	1	10	2.574	16	2.570	3	3	1
35	4.754	26	4.749	1	0	$\bar{3}$			7	2.531	4	$\bar{1}$	$\bar{4}$
		38	4.749	1	0	3			5	2.530	4	1	4
25	4.628	42	4.620	0	2	0			7	2.509	0	0	6
10	4.579	12	4.573	2	1	$\bar{2}$	20	2.474	12	2.472	3	1	5
		12	4.573	2	1	2			5	2.450	5	2	$\bar{1}$
10	4.416	8	4.417	0	2	1			5	2.386	2	2	5
		17	4.408	1	2	0	25	2.376	31	2.375	2	0	$\bar{6}$
5	4.170	5	4.165	3	$\bar{1}$	$\bar{1}$			19	2.374	2	0	6
		9	4.165	3	1	1			8	2.310	0	4	0
40	3.934	32	3.937	0	2	2			5	2.267	2	3	$\bar{4}$
5	3.800	9	3.804	1	2	$\bar{2}$			5	2.267	2	3	4
		9	3.804	1	2	2			7	2.259	4	1	5
5	3.751	9	3.756	3	1	$\bar{2}$	15	2.184	5	2.181	2	4	1
45	3.510	25	3.509	3	0	$\bar{3}$	15	2.142	5	2.144	6	1	3
		57	3.508	3	0	3			6	2.137	4	3	3
		8	3.485	0	1	4	10	2.109	8	2.107	2	3	$\bar{1}$
		7	3.472	2	$\bar{2}$	$\bar{2}$			8	2.105	5	0	5
15	3.392	19	3.399	0	2	3	10	2.078	9	2.077	1	$\bar{4}$	$\bar{3}$
		5	3.392	1	$\bar{1}$	$\bar{4}$	10	2.047	7	2.048	5	3	2
		7	3.364	3	2	0	10	2.02	7	2.018	2	4	$\bar{3}$
10	3.345	12	3.351	2	0	$\bar{4}$			6	1.970	3	0	$\bar{7}$
35	3.336	46	3.334	4	1	$\bar{1}$			5	1.940	7	0	3
			3.334	4	1	1			5	1.926	3	$\bar{1}$	$\bar{7}$
15	3.310	18	3.312	1	2	3	15	1.840	27	1.840	8	0	0
		10	3.307	4	0	$\bar{2}$	5	1.802	4	1.804	5	4	1
		5	3.306	4	0	2	5	1.720	5	1.718	3	$\bar{5}$	$\bar{1}$
5	3.288	10	3.283	3	2	$\bar{1}$	5	1.684	5	1.692	7	$\bar{3}$	2
		5	3.283	3	2	1			5	1.662	1	0	9
		16	3.280	3	$\bar{1}$	$\bar{3}$			5	1.640	6	$\bar{2}$	$\bar{6}$
10	3.154	18	3.150	2	$\bar{1}$	$\bar{4}$			5	1.640	6	2	$\bar{6}$
		12	3.150	2	1	4	5	1.557	5	1.5568	5	$\bar{5}$	1
10	3.118	17	3.113	4	$\bar{1}$	$\bar{2}$	5	1.502	7	1.5052	0	0	10
		16	3.113	4	1	2	5	1.449	5	1.4485	6	5	2
		5	3.018	0	3	1	5	1.241	5	1.2412	4	5	$\bar{8}$
15	2.880	19	2.879	4	2	0							

Intensities estimated visually. I_{calc} calculated with program *LAZY PULVERIX* (Yvon *et al*., 1977); only reflections with I_{calc} >4 are listed.

X-ray powder diffraction data

X-ray powder-diffraction data (Table 2) were obtained using a 100 mm Guinier-Hägg camera using Cu$K\alpha$ radiation (λ 1.54060 Å) and silicon (NBS SRM 640a) as an internal standard. Intensities were estimated visually and the calculated intensities were obtained from the structural model (Yvon *et al*., 1977). The Guinier-Hägg film was scanned using an Epson film scanner, the powder-diffraction profile over the 2θ range 10 to 90º was extracted and the unit-cell parameters were refined using the Le Bail profile-fitting method (Le Bail *et al*., 1988; Hunter, 1998) starting from the unit-cell parameters determined from single-crystal techniques. The unit-cell parameters refined from the powder data are a = 14.716(2), b = 9.247(2), c = 15.034(2) Å, β = 89.89(2)º, V = 2045.9(2) Å^3, which agree with those refined using single-crystal methods.

Infrared spectroscopy

The infrared spectrum (Fig. 2) of hylbrownite was obtained using a Nicolet 5700 FTIR spectrometer equipped with a Nicolet Continuum IR microscope and a diamond-anvil cell. A crystal aggregate was crushed in the diamond cell and a spectrum recorded in the range 4000 to 650 cm^{-1}.

TABLE 3. Crystal data, data collection and refinement details.

Crystal data	
Space group	$P2_1/n$
a,b,c (Å)	14.722(3), 9.2400(18), 15.052(3)
β (º)	90.01(3)
V (Å^3), Z	2047.5(7), 4
F(000)	1151.0
μ (mm^{-1})	0.474
Crystal dimensions (mm)	0.055 × 0.006 × 0.006
Data collection	
Diffractometer	ADSC Quantum 210r
Temperature (K)	123
Wavelength	0.774867 Å
θ range (º)	10.63−23.10
Detector distance (mm)	85.32
Rotation axes	ϕ, ω
Rotation width (º)	2.0
Total no. of frames	180
Collection time per frame (s)	10
h,k,l ranges	−16 → 16, –9 → 9, –16 → 16
Total reflections measured	21200
Unique reflections	2417 (R_{int} = 0.0373)
Refinement	
Refinement on	F^2
$R1$* for $F_0 > 4\sigma(F_0)$	4.50%
w$R2$† for all F_0^2	10.70%
Reflections used $F_o > 4\sigma(F_o)$	2313
Number of parameters refined	344
Extinction factor	0.016(2)
$(\Delta/\sigma)_{max}$	0.000
$\Delta\rho$min, $\Delta\rho$max (e/Å^3)	0.361, -0.399
GoF	1.086

* $R1 = \Sigma||Fo|-|Fc|| / \Sigma|Fo|$

† $wR2 = \Sigma w(|Fo|^2-|Fc|^2)^2 / \Sigma w|Fo|^2)^{1/2}$; w = 1/[$\sigma^2(F o^2)$ + (0.042 P)^2 + 12.60 P]; P = ([max of (0 or F_0^2)] + 2Fc^2)/3

TABLE 4. Fractional atomic coordinates and displacement parameters (in Å^2) for hylbrownite.

Atom	x	y	z	U_{eq}	U_{11}	U_{22}	U_{33}	U_{12}	U_{13}	U_{23}
Na1	0.64272(12)	0.5333(2)	0.70920(11)	0.0138(10)	0.0108(13)	0.0152(14)	0.0153(13)	0.0010(7)	0.0016(7)	0.0002(7)
Na2	0.74705(12)	0.2664(2)	0.43719(11)	0.0157(10)	0.0136(13)	0.0156(15)	0.0180(13)	0.0028(7)	0.0008(7)	–0.0001(7)
Na3	0.88656(12)	0.6910(2)	0.70257(12)	0.0184(11)	0.0094(13)	0.0256(16)	0.0200(14)	–0.0060(8)	0.0013(7)	–0.0015(8)
Mg	0.74842(9)	0.54443(15)	0.32017(9)	0.0093(8)	0.0064(10)	0.0095(11)	0.0121(10)	0.0000(5)	0.0014(5)	0.0002(5)
P1	0.90421(7)	0.77053(13)	0.40312(7)	0.0087(7)	0.0058(9)	0.0097(10)	0.0108(9)	0.0008(5)	0.0012(4)	0.0002(4)
P2	0.60850(7)	0.77852(13)	0.40899(7)	0.0097(7)	0.0071(9)	0.0102(10)	0.0117(9)	0.0002(4)	0.0007(4)	0.0014(4)
P3	0.75830(8)	0.65684(13)	0.51764(7)	0.0105(7)	0.0087(9)	0.0119(10)	0.0110(9)	0.0000(5)	0.0010(4)	–0.0006(5)
O1	0.9041(2)	0.9333(4)	0.3925(2)	0.0139(8)	0.0152(16)	0.0090(19)	0.0175(16)	0.0010(13)	0.0020(12)	–0.0010(13)
O2	0.8513(2)	0.6951(4)	0.3300(2)	0.0140(8)	0.0113(16)	0.0156(19)	0.0149(16)	0.0010(13)	0.0014(12)	0.0004(13)
O3	0.9984(2)	0.7073(4)	0.4202(2)	0.0175(8)	0.0100(16)	0.019(2)	0.0230(18)	–0.0007(14)	–0.0010(13)	0.0014(13)
O4	0.8518(2)	0.7380(4)	0.4966(2)	0.0168(8)	0.0133(17)	0.023(2)	0.0141(16)	–0.0016(14)	0.0033(12)	–0.0072(14)
O5	0.5252(2)	0.7074(4)	0.4476(2)	0.0183(8)	0.0128(16)	0.018(2)	0.0238(18)	0.0013(14)	0.0066(13)	–0.0004(13)
O6	0.5977(2)	0.9384(4)	0.3898(2)	0.0148(8)	0.0141(17)	0.0127(19)	0.0175(16)	0.0010(13)	0.0009(12)	0.0000(13)
O7	0.6457(2)	0.6944(4)	0.3290(2)	0.0148(8)	0.0123(16)	0.017(2)	0.0148(16)	–0.0007(13)	0.0006(12)	–0.0010(13)
O8	0.6860(2)	0.7753(4)	0.4867(2)	0.0203(9)	0.0190(18)	0.023(2)	0.0186(17)	–0.0044(14)	–0.0037(13)	0.0058(14)
O9	0.7540(2)	0.6445(4)	0.6157(2)	0.0150(8)	0.0128(16)	0.016(2)	0.0157(16)	–0.0013(13)	0.0007(12)	–0.0023(13)
O10	0.7490(2)	0.5251(4)	0.4610(2)	0.0149(8)	0.0110(16)	0.0158(19)	0.0180(17)	0.0015(13)	0.0012(12)	–0.0020(13)
OW11	0.7490(2)	0.5533(4)	0.1812(2)	0.0154(8)	0.0133(17)	0.0120(19)	0.0208(17)	–0.0009(13)	0.0034(13)	–0.0012(13)
OW12	0.8401(2)	0.3690(4)	0.3207(2)	0.0154(8)	0.0105(17)	0.022(2)	0.0142(16)	–0.0030(14)	0.0017(12)	–0.0021(13)
OW13	0.6508(2)	0.3719(4)	0.3205(2)	0.0171(8)	0.0135(17)	0.022(2)	0.0157(17)	–0.0021(14)	0.0012(13)	0.0013(14)
OW14	0.6202(2)	0.7627(4)	0.7783(2)	0.0201(8)	0.0141(17)	0.025(2)	0.0208(18)	0.0008(15)	0.0049(13)	0.0017(14)
OW15	0.8031(2)	0.7945(4)	0.8246(2)	0.0191(8)	0.0162(18)	0.018(2)	0.0228(18)	0.0020(14)	0.0023(14)	–0.0004(14)
OW16	0.5170(2)	0.5665(4)	0.6092(2)	0.0172(8)	0.0151(17)	0.020(2)	0.0169(17)	0.0013(14)	–0.0010(13)	–0.0016(14)
OW17	0.7239(3)	0.4710(4)	0.8428(2)	0.0257(9)	0.033(2)	0.023(2)	0.0216(19)	0.0026(15)	0.0016(15)	0.0050(16)
OW18	0.9873(2)	0.8923(4)	0.7176(2)	0.0186(8)	0.0155(17)	0.019(2)	0.0208(18)	–0.0002(14)	0.0028(13)	–0.0003(14)
OW19	0.8563(2)	0.1326(4)	0.5159(2)	0.0177(8)	0.0135(17)	0.020(2)	0.0194(17)	–0.0023(14)	0.0009(13)	0.0017(14)
OW20	0.6298(2)	0.1489(4)	0.5161(2)	0.0177(8)	0.0136(17)	0.021(2)	0.0188(17)	–0.0036(14)	0.0019(13)	0.0002(14)
OW21	0.9944(2)	0.5834(4)	0.6054(2)	0.0181(8)	0.0169(17)	0.016(2)	0.0211(18)	–0.0009(14)	–0.0015(13)	0.0017(14)
OW22	0.9307(2)	0.5118(4)	0.8120(2)	0.0217(9)	0.0146(18)	0.021(2)	0.0291(19)	–0.0036(15)	0.0003(14)	–0.0003(14)
H1	0.696(3)	0.507(7)	0.163(4)	0.041(4)*						
H2	0.796(3)	0.513(7)	0.146(4)	0.041(4)*						
H3	0.901(3)	0.374(8)	0.341(4)	0.041(4)*						
H4	0.841(4)	0.308(7)	0.271(4)	0.041(4)*						
H5	0.642(4)	0.309(7)	0.274(4)	0.041(4)*						
H6	0.593(3)	0.393(8)	0.342(4)	0.041(4)*						
H7	0.602(5)	0.839(6)	0.741(4)	0.041(4)*						
H8	0.575(4)	0.749(7)	0.820(4)	0.041(4)*						

H9	0.817(4)	0.746(7)	0.876(4)	0.041(4)*
H10	0.740(3)	0.795(8)	0.817(4)	0.041(4)*
H11	0.521(5)	0.624(6)	0.559(4)	0.041(4)*
H12	0.499(5)	0.477(5)	0.592(4)	0.041(4)*
H13	0.698(4)	0.516(7)	0.891(4)	0.041(4)*
H14	0.750(4)	0.386(6)	0.866(4)	0.041(4)*
H15	1.025(4)	0.883(8)	0.767(3)	0.041(4)*
H16	1.018(4)	0.947(7)	0.675(3)	0.041(4)*
H17	0.914(4)	0.179(7)	0.538(4)	0.041(4)*
H18	0.886(4)	0.061(6)	0.481(4)	0.041(4)*
H19	0.616(4)	0.065(6)	0.485(4)	0.041(4)*
H20	0.571(4)	0.193(7)	0.524(4)	0.041(4)*
H21	0.989(5)	0.617(6)	0.548(3)	0.041(4)*
H22	0.989(7)	0.481(5)	0.598(5)	0.041(4)*
H23	0.990(3)	0.530(11)	0.834(5)	0.041(4)*
H24	0.895(4)	0.528(11)	0.863(4)	0.041(4)*

* constrained to be equal during refinement.

The spectrum shows PO_4 vibrational modes analogous to those for other condensed phosphates (e.g. Rulmont *et al*., 1991); asymmetric stretching vibrations of PO_3 groups (at 1254, 1118, 1022, 995 and 906 cm^{-1}), O−P−O stretching vibrations (at 742 and 906 cm^{-1}), O−P−O bending vibrations (at 692 and 658 cm^{-1}). A prominent band centred on 3278 cm^{-1} is due to OH-stretching vibrations and bands at 1670 and 1643 cm^{-1} correspond to H−O−H-bending of H_2O groups. Based on the correlation between O−H-stretching frequences (νOH) and O−H...O distances (Libowitzky, 1999), νOH values from ~3179 to 3573 cm^{-1} are predicted for hylbrownite, which fall within the range of observed values.

Crystal structure solution and refinement

Single-crystal X-ray data collection

X-ray data were collected at the Australian Synchrotron facility using an ADSC Quantum 210r detector. Data were measured using a crystal of dimensions $0.055 \times 0.006 \times 0.006$ mm, with monochromatic Mo$K\alpha$ X-radiation (λ = 0.774867 Å), a crystal-to-detector distance of 85 mm and by scanning in ϕ and ω with frame widths of 2º and 10 s spent counting per frame. Data were integrated and corrected for Lorentz, polarization and background effects. Normalized structure-factor statistics and systematic absences indicated space group $P2_1/n$, with verification provided by the successful solution of the structure. Crystal structure solution by direct methods using *SHELXS-97* (Sheldrick, 2008) found the positions of three Na, one Mg and three P atoms. Fourier and difference Fourier syntheses (SHELXL-97, Sheldrick, 2008) located the positions of 22 O atoms and subsequent difference Fourier maps revealed all 24 H atoms belonging to the water molecules. The O−H distances were restrained to 0.95 Å and H−H distances of water molecules were restrained to 1.50 Å, in each case with standard deviations of 0.05. A full-matrix least-squares refinement on F^2 with anisotropic displacement parameters for all non-H atoms converged to an R_1 of 4.50%. Table 3 contains data-collection parameters and refinement results, Table 4 lists the atom coordinates and displacement parameters for all atoms, Table 5 gives selected interatomic and Table 6 lists the calculated bond-valence sums (Brown and Altermatt, 1985; Brown, 1996).

TABLE 5. Selected interatomic distances (Å) for hylbrownite.

Na1	OW14	2.384(4)	Mg	O7	2.056(4)
	O9	2.392(4)		O2	2.063(3)
	OW15	2.401(4)		OW11	2.093(3)
	OW16	2.406(4)		OW12	2.109(4)
	OW17	2.408(4)		OW10	2.127(3)
	OW18	2.565(4)		OW13	2.146(4)
	<Na–O>	2.426		<Mg–O>	2.099
Na2	O21	2.377(4)	P1	O1	1.513(4)
	O9	2.387(4)		O2	1.518(3)
	OW18	2.390(4)		O3	1.527(3)
	OW15	2.408(4)		O4	1.633(3)
	O22	2.424(4)		<P–O>	1.548
	OW17	3.131(4)			
	O4	3.172(4)	P2	O5	1.507(4)
	<Na–O>	2.613		O6	1.513(4)
				O7	1.534(3)
Na3	OW19	2.349(4)		O8	1.634(3)
	O20	2.359(4)		<P–O>	1.547
	OW10	2.418(4)			
	OW12	2.419(4)	P3	O9	1.482(3)
	OW13	2.458(4)		OW10	1.493(4)
	OW11	2.657(4)		O8	1.596(4)
	<Na–O>	2.443		O4	1.600(3)
				<P–O>	1.543
O2–Mg–OW11		92.42(14)	O5–P2–O6		114.44(19)
O2–Mg–OW12		92.79(13)	O5–P2–O7		111.83(19)
O2–Mg–OW10		89.00(13)	O5–P2–O8		106.53(19)
O7–Mg–O2		94.61(14)	O6–P2–O7		112.46(18)
O7–Mg–OW11		92.37(14)	O6–P2–O8		103.15(19)
O7–Mg–OW10		89.70(13)	O7–P2–O8		107.64(17)
O7–Mg–OW13		90.46(14)	<O–P2–O>		109.34
OW10–Mg–OW13		86.44(13)			
OW11–Mg–OW12		91.77(13)			
OW11–Mg–OW13		91.95(13)	O8–P3–O4		101.23(19)
OW12–Mg–OW10		85.97(13)	O9–P3–O4		105.66(17)
OW12–Mg–OW13		81.81(14)	O9–P3–O8		108.37(18)
<O–Mg–O>		89.94	O9–P3–OW10		120.18(19)
			OW10–P3–O8		109.33(18)
O1–P1–O2		112.31(18)	OW10–P3–O4		110.38(18)
O1–P1–O3		113.49(19)	<O–P3–O>		109.19
O1–P1–O4		105.89(18)			
O2–P1–O3		114.36(19)			
O2–P1–O4		107.35(17)			
O3–P1–O4		102.35(18)			
<O–P1–O>		109.29			

Description of the structure

The hylbrownite structure contains three unique Na atoms, one Mg atom and three P atoms. The Na1 and Na3 atoms are each [6]-coordinated by five H_2O groups and one O^{2-} anion to form distorted $[Na(H_2O)_5O]$ octahedra. The octahedra are highly distorted, with intra-octahedral angles deviating by 14.7º and 26.0º from ideal angles for the Na1 and Na3 sites respectively. The Na2 atom is coordinated by four H_2O groups and one O^{2-} anion forming "strong" bonds, with Na–O distances in

TABLE 6. Bond-valence analysis for hylbrownite.

	Na1	Na2	Na3	Mg	P1	P2	P3	H1	H2	H3	H4	H5	H6	H7	H8	H9	H10	H11	H12	H13	H14	H15	H16	H17	H18	H19	H20	H21	H22	H23	H24	Sum
O1					1.33			0.18															0.16		0.19							1.86
O2				0.37	1.31							0.16																				1.84
O3					1.28										0.15									0.20				0.10	0.21			1.94
O4					0.96		1.05																					0.06				2.07
O5						1.35												0.17	0.17								0.21					1.90
O6						1.33			0.20																	0.17				0.18		1.88
O7				0.38		1.25					0.17											0.09										1.89
O8						0.96	1.06																									2.02
O9	0.20	0.21					1.44														0.08											1.93
O10			0.19	0.31			1.40																									1.90
OW11			0.10	0.34				0.82	0.80																							2.06
OW12			0.19	0.33						0.80	0.83																					2.15
OW13			0.17	0.29								0.84	0.82																			2.12
OW14	0.21													0.83	0.85		0.16															2.05
OW15	0.20	0.20														0.86	0.84															2.10
OW16	0.20												0.18					0.83	0.83													2.04
OW17	0.20																			0.86	0.92										0.04	2.02
OW18	0.13	0.21																				0.91	0.84									2.09
OW19			0.23																	0.14				0.80	0.81							1.98
OW20			0.23													0.14										0.83	0.79				0.13	2.12
OW21		0.21								0.20																		0.84	0.79			2.04
OW22		0.19												0.17																0.82	0.83	2.01
Sum	1.14	1.02	1.11	2.02	4.88	4.89	4.95	1.00	1.00	1.00	1.00	1.00	1.00	1.00	1.00	1.00	1.00	1.00	1.00	1.00	1.00	1.00	1.00	1.00	1.00	1.00	1.00	1.00	1.00	1.00	1.00	

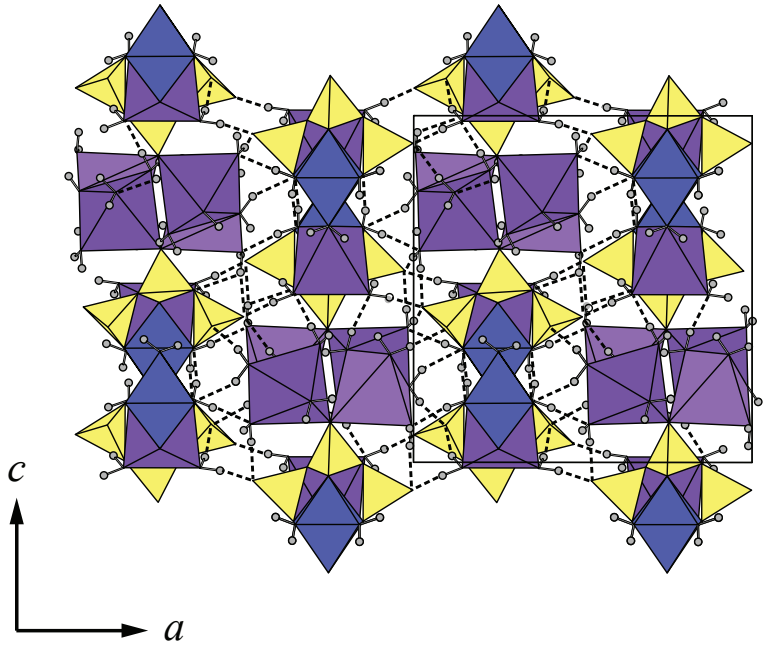

FIG. 3. The crystal structure of hylbrownite viewed along [010]; Naϕ_6 octahedra are dark purple; Naϕ_5 polyhedra are pale purple; Mgϕ_6 octahedra are blue; PO_4 tetrahedra are yellow; H atoms are shaded grey. The unit cell is outlined. Hydrogen bonds are shown as dotted lines. All structure drawings were completed using *ATOMS* (Shape Software 1997).

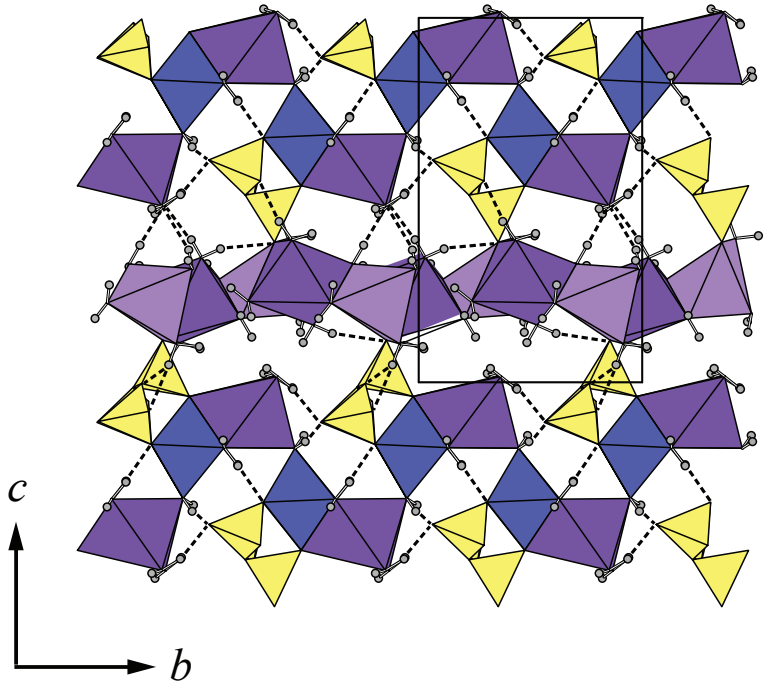

FIG. 4. The crystal structure of hylbrownite viewed along [100]. Legend as in Fig. 3.

the range 2.377(4)−2.424(4) Å (Table 5). The Na2 atom is also weakly bonded to two anions, with Na−O distances of 3.131(4) and 3.172(4) Å.

The Mg site is coordinated by four H_2O groups and two O atoms in an octahedral arrangement. The $[Mg(H_2O)_4O_2]$ octahedron is reasonably regular in geometry, with Mg−O distances in the range 2.056 to 2.146 Å and angles in the range 81.81 to 94.61º.

The Mg site refines to slightly greater than full occupancy [1.025(14)] and the Na sites to slightly less than full occupancy (0.955(14), 0.986(15) and 0.949(15) for Na1, Na2 and Na3 respectively), suggesting that the minor Ca detected in the chemical analysis is located at the Mg site.

The P1, P2 and P3 sites are each tetrahedrally coordinated by four O atoms, at mean distances of 1.548, 1.547 and 1.543 Å respectively. The three PO_4 tetrahedra form a P_3O_{10} trimer by the sharing of vertices, with the $P1O_4$ and $P3O_4$ tetrahedra sharing the O4 vertex and the $P2O_4$ and $P3O_4$ tetrahedra sharing the O8 vertex. The PO_4 tetrahedra, in particular the $P3O_4$ tetrahedron, show considerable angular distortion (Table 5). The P1 and P2 cations coordinate to three and the P3 cation to two non-bridging O atoms with P−O distances of 1.482(3) to 1.534(3) Å and to one (P1 and P2) or two (P3) bridging O atoms with longer P−O distances (1.596(4), 1.600(3), 1.633(3) and 1.634(3) Å). The bridging anions, O4 and O8, are each bonded to two P atoms hence require less than the average P−O bond-valence of 1.25 v.u. from each bridging bond which are, as a consequence, significanly longer than the terminal P−O bonds.

Each PO_4 tetrahedron shares one vertex with a $Mg\phi_6$ octahedron to form an $[Mg(H_2O)_3P_3O_{10}]$ cluster (Fig. 3). The $Mg\phi_6$ octahedron shares a face with an $Na3\phi_6$ octahedron, which also links

TABLE 7. Details of hydrogen bonding in hylbrownite (Å, º).

D−H···*A*	*D*−H	H···*A*	*D*···*A*	∠*D*−H···*A*
O11–H1...O1^{i}	0.94(4)	1.82(5)	2.746(4)	170(6)
O11–H2...O6^{i}	0.95(4)	1.80(4)	2.714(4)	163(6)
O12–H3...O21^{ii}	0.94(4)	1.79(4)	2.715(5)	167(6)
O12–H4...O7^{i}	0.93(4)	1.85(4)	2.779(4)	175(6)
O13–H5...O2^{i}	0.93(4)	1.88(4)	2.793(4)	168(6)
O13–H6...O16^{iii}	0.93(4)	1.82(4)	2.747(5)	176(6)
O14–H7...O22^{iv}	0.94(4)	1.85(5)	2.776(5)	169(7)
O14–H8...O3^{v}	0.93(4)	1.92(5)	2.802(5)	158(6)
O15–H9...O20^{iv}	0.92(4)	2.01(4)	2.920(5)	170(6)
O15–H10...O14	0.93(4)	1.89(4)	2.798(5)	166(7)
O16–H11...O5	0.92(4)	1.85(5)	2.762(5)	170(6)
O16–H12...O5^{iii}	0.91(4)	1.84(5)	2.742(5)	174(7)
O17–H13...O19^{iv}	0.92(4)	1.94(4)	2.854(5)	172(6)
O17–H14...O9^{vi}	0.94(4)	2.25(5)	3.098(5)	150(6)
O18–H15...O7^{vii}	0.93(4)	2.13(5)	2.982(5)	152(6)
O18–H16...O1^{viii}	0.93(4)	1.89(5)	2.810(5)	169(6)
O19–H17...O3^{ii}	0.97(4)	1.78(4)	2.773(5)	168(6)
O19–H18...O1^{ix}	0.95(4)	1.80(4)	2.709(5)	159(6)
O20–H19...O6^{ix}	0.93(4)	1.86(5)	2.761(5)	160(7)
O20–H20...O5^{iii}	0.97(4)	1.74(4)	2.697(5)	169(6)
O21–H21...O3	0.93(4)	2.10(4)	3.014(5)	170(6)
O21–H21...O4	0.93(4)	2.43(6)	3.020(5)	122(5)
O21–H22...O3^{ii}	0.95(5)	1.77(5)	2.716(5)	170(9)
O22–H23...O6^{vii}	0.94(5)	1.82(5)	2.762(5)	173(7)
O22–H24...O20^{iv}	0.95(5)	2.16(6)	3.015(5)	149(7)
O22–H24...O17	0.95(5)	2.59(7)	3.103(5)	114(6)

Symmetry codes: (i) $-x+3/2$, $y-1/2$, $-z+1/2$; (ii) $-x+2$, $-y+1$, $-z+1$; (iii) eqiv $6 $-x+1$, $-y+1$, $-z+1$; (iv) $-x+3/2$, $y+1/2$, $-z+3/2$; (v) $x-1/2$, $-y+3/2$, $z+1/2$; (vi) $-x+3/2$, $y-1/2$, $-z+3/2$; (vii) $x+1/2$, $-y+3/2$, $z+1/2$; (viii) $-x+2$, $-y+2$, $-z+1$; (ix) x, $y-1$, z

to other $[Mg(H_2O)_3P_3O_{10}]$ cluster, in the *c* direction, via corner-sharing. Na1ϕ_6 octahedra and Na2ϕ_5 polyhedra share edges to form Na_2O_9 groups, which link via corners (the O9 anion) to form a chain with a staggered geometry that extends along the *b* direction (Fig. 4). The chains of Na_2O_9 groups link the $[Mg(H_2O)_3P_3O_{10}]$ clusters in the *c* direction, *via* corner-sharing, to form a thick sheet parallel to (100). Linkage in the *a* direction is via hydrogen bonds only.

Hydrogen bonding

All O atoms not bonded to P are in H_2O groups. All H_2O groups are hydrogen-bond donors and OW14, OW16, OW17, OW19, OW20, OW21 and OW22 are both hydrogen-bond donors and hydrogen-bond acceptors. Incident bond-valence sums (Table 6) indicate that six of the eight anions bonded to P must be hydrogen-bond acceptors. An extensive network of hydrogen bonds (Figs 3, 4) can be divided into those within the sheets and those that provide linkage between the sheets. Details of the hydrogen bonding is given in Table 7. Hydrogen bonds between the sheets, directed toward the O1, O3, O5 and O6 atoms of the P_3O_{10} trimer adjacent in the *a* direction, are provided by H8, H12, H16, H17, H20, H22 and H23. Further hydrogen bonds between the sheets are provided by H3, H6 and H15, which hydrogen bond to OW21, OW16 and O7, respectively. The remaining hydrogen bonds occur within the sheets. Bifurcated H-bonds are provided by the H21 atom of OW21, to adjacent O3 and O4 anions, and by the H24 atom of OW22, to adjacent O17 and O20 anions. All hydrogen bonds are medium strong to very weak in strength, with O...O distances between 2.697(5) and 3.103(5) Å (Libowitzky, 1999).

Relationships to other minerals and inorganic compounds

Hylbrownite is the Mg analogue of kanonerovite, $MnNa_3P_3O_{10}{\cdot}12H_2O$, (Popova *et al.*, 2002) (Table 8). No structural study of kanonerovite has been completed; however, the structure of synthetic $MnNa_3P_3O_{10}{\cdot}12H_2O$ is known (Lightfoot and Cheetham, 1987). In the literature, two other crystal-structure refinements of $M^{2+}Na_3P_3O_{10}{\cdot}12H_2O$-type compounds are available; $CdNa_3P_3O_{10}{\cdot}12H_2O$ (Lutsko and Johansson, 1984) and $CuNa_3P_3O_{10}{\cdot}12H_2O$ (Jouini *et al*., 1984). As was mentioned above, hylbrownite is

TABLE 8. Comparison of related minerals and compounds.

Mineral name	Hylbrownite	Kanonerovite						
Formula	$MgNa_3P_3O_{10}$ ·$12H_2O$	$MnNa_3P_3O_{10}$ ·$12H_2O$	$CuNa_3P_3O_{10}$ ·$12H_2O$	$CdNa_3P_3O_{10}$ ·$12H_2O$	$NiNa_3P_3O_{10}$ ·$12H_2O$	$ZnNa_3P_3O_{10}$ ·$12H_2O$	$MnNa_3P_3O_{10}$ ·$12H_2O$	$CoNa_3P_3O_{10}$ ·$12H_2O$
Crystal system	monoclinic	monoclinic	monoclinic	monoclinic	monoclinic	monoclinic	monoclinic	monoclinic
Space group	$P2_1/n$	$P2_1/n$	$P2_1/n$	$P2_1/n$	$P2_1/n$	$P2_1/n$	$P2_1/n$	$P2_1/n$
a (Å)	14.722(3)	14.71(1)	15.052(8)	14.835(12)	15.01	15.03	15.13	15.06
b (Å)	9.240(2)	9.33(1)	9.234(3)	9.397(10)	9.208	9.241	9.320	9.238
c (Å)	15.052(3)	15.13(2)	14.767(8)	15.244(9)	14.71	14.70	14.76	14.70
β (°)	90.01(3)	89.8(1)	90.03(5)	90.20(6)	90	90	90	90
V (Å^3)	2047.5(7)	2075(3)	2052.47	2125.07	2033.1	2041.7	2081.3	2045.1
Z	4	4	4	4	4	4	4	4
Reference	this work	Popova *et al.* (2002)	Jouini *et al.* (1984)	Lutsko and Johansson (1984)	Rakotomahanina *et al.* (1972)	Rakotomahanina *et al.* (1972)	Rakotomahanina *et al.* (1972)	Rakotomahanina *et al.* (1972)

the natural analogue of $MgNa_3P_3O_{10}\cdot12H_2O$, a synthetic compound that was synthesized by Rakotomahanina *et al.*, (1972) along with other triphosphates of the type $M^{2+}Na_3P_3O_{10}\cdot12H_2O$, with M^{2+} = Ni, Co, Mn, Zn and Cd. Unit-cell parameters for these compounds were refined from powder X-ray diffraction data (Table 8), however, they were not characterized structurally. Hylbrownite is the fourth example of a condensed phosphate mineral after kanonerovite (Popova *et al.*, 2002), and the pyrophosphates canaphite $CaNa_2P_2O_7\cdot4H_2O$ (Peacor *et al*., 1985; Rouse *et al*., 1988) and wooldridgeite $Na_2CaCu_{22}(P_2O_7)_2\cdot10H_2O$ (Hawthorne *et al*., 1999; Cooper and Hawthorne, 1999). Hylbrownite is the third known phosphate of Na and Mg, after panethite, $(Na,Ca,K)_4(Mg,Fe^{2+},Mn)_4(PO_4)_2$, (Fuchs *et al*., 1967) and bakhchisaraitsevite, $[Na_2(H_2O)_2]\{(Mg,Fe)_5(H_2O)_5(PO_4)_4\}$ (Liferovich *et al*., 2000; Yakubovich *et al*., 2000).

Acknowledgements

The specimen containing hylbrownite was kindly provided by Bill Aird. We thank Angus Netting and John Terlet of Adelaide Microscopy, The University of Adelaide for assistance with the microprobe analysis and Hayley Brown, of the Forensic Science Centre, Adelaide, with collection of the infrared spectrum. The manuscript benefited from reviews by Igor Pekov and an anonymous reviewer.

References

Bayliss, P., Lawrence, L.J. and Watson, D. (1966) Rare copper arsenates from Dome Rock, South Australia. *Australian Journal of Science*, **29**, 145–146.

Brown, H.Y.L. (1893) *Catalogue of South Australian minerals: with the mines and other localities where found, and brief remarks on the mode of occurrence of some of the principal metals and ores*. Government Printer, Adelaide, 34 pp.

Brown, H.Y.L. (1908) *Record of the Mines of South Australia, 4th ed*. Government Printer, Adelaide, 382 pp.

Brown, I.D. (1996) *VALENCE*: a program for calculating bond-valences. *Journal of Applied Crystallography*, **29**, 479–480.

Brown, I.D. and Altermatt, D. (1985) Bond-valence parameters obtained from a systematic analysis of the inorganic crystal structure database. *Acta Crystallographica*, **B41**, 244–247.

Cooper, M.A. and Hawthorne, F.C. (1999) The crystal structure of wooldridgeite, $Na_2CaCu_2^{2+}(P_2O_7)_2(H_2O)_{10}$, a novel copper pyrophosphate mineral. *The Canadian Mineralogist*, **37**, 73–81.

Dickinson, S.B. (1942) The structural control of ore deposition in some South Australian copperfields. *Geological Survey of South Australia Bulletin* **20**, 1–39.

Fuchs, L.H., Olsen, E. and Henderson, E.P. (1967) On the occurrence of brianite and panethite, two new phosphate minerals from the Dayton meteorite, *Geochimica et Cosmochimica Acta*, **31**, 1711–1719.

Hawthorne, F.C., Cooper, M.A., Green, D.I., Starkey, R.E., Roberts, A.C. and Grice, J.D. (1999) Wooldridgeite, $Na_2CaCu_2^{2+}(P_2O_7)_2(H_2O)_{10}$: a new mineral from Judkins Quarry, Warwickshire, England. *Mineralogical Magazine*, **63**, 13–16.

Hunter, B.A. (1998) Rietica – A Visual Rietveld Program. *Commission on Powder Diffraction Newsletter*, **20**, 21.

Jouini, O., Dabbabi, M., Averbuch-Pouchot, M.T., Guitel, J.C. and Durif, A. (1984) Structure du phosphate de cuivre(II) et de trisodium dodecahydrate, $CuNa_3P_3O_{10}(H_2O)_{12}$. *Acta Crystallographica*, **C40**, 728–730.

Kleeman, A.W. and Milnes, A.R. (1973) Phosphorian lavendulan from Dome Rock mine, South Australia. *Transactions of the Royal Society of South Australia*, **97**, 135–137.

Le Bail, A., Duroy, H., Fourquet, J.L. (1988) Ab-initio structure determination of $LiSbWO_6$ by X-ray powder diffraction. *Materials Research Bulletin* **23**, 447–452.

Libowitzky, E. (1999) Correlation of O-H stretching frequencies and O-H···O hydrogen bond lengths in minerals. *Monatshefte für Chemie*, **130**, 1047–1059.

Liferovich, R.P., Pakhomovsky, Ya.A., Yakubovich, O.V., Massa, W., Laajoki, K., Gehör, S., Bogdanova, A.N. and Sorokhtina, N.V. (2000) Bakhchisaraitsevite, $Na_2Mg_5[PO_4]_4\cdot7H_2O$, a new mineral from hydrothermal assemblages related to phoscorite–carbonatite complex of the Kovdor massif, Russia. *Neues Jahrbuch für Mineralogie, Monatshefte*, 402–418.

Lightfoot, P. and Cheetham, A.K. (1987) Structure of manganese(II) trisodium tripolyphosphate dodecahydrate. *Acta Crystallographica*, **C43**, 4–7.

Lutsko, V. and Johansson, G. (1984) The crystal structure of trisodium cadmium triphosphate $CdNa_3P_3O_{10}(H_2O)_{12}$. *Acta Chemica Scandinavica*, **A38**, 415–417

Mandarino, J.A. (1981) The Gladstone-Dale relationship: Part IV: The compatibility concept and its application. *The Canadian Mineralogist*, **19**, 441–450.

Nickel, E.H. and Birch, W.D. (1988) Cobaltaustinite – a new arsenate mineral from Dome Rock, South Australia. *Australian Mineralogist*, **3**, 53–57.

Peacor, D.R., Dunn, P.J., Simmons,W.B. and Wicks, F.J. (1985) Canaphite, a new sodium calcium phosphate from the Paterson area, New Jersey. *Mineralogical Record*, **16**, 467–468.

Popova, V.I., Popov, V.A., Sokolova, E.V., Ferraris, G. and Chukanov, N.V. (2002) Kanonerovite, $MnNa_3P_3O_{10}\cdot 12H_2O$, first triphosphate mineral (Kazennitsa pegmatite, Middle Urals, Russia). *Neues Jahrbuch für Mineralogie, Monatshefte*, 117–127.

Pouchou, J.L. and Pichoir, F. (1985) 'PAP' $\phi((\rho Z))$ procedure for improved quantitative microanalysis. Pp. 104–106 in: *Microbeam Analysis* (J.T. Armstrong, editor). San Francisco Press, San Francisco, California.

Rakotomahanina, E., Averbuch-Pouchot, M.-T. and Durif, A. (1972) Données cristallographiques sur les triphosphates du type $M^{II}Na_3P_3O_{10}\cdot 12H_2O$ pour M^{II} = Ni, Co, Mn, Mg, Zn et Cd. *Bulletin Société Français de Minéralogie et de Cristallographie*, **95**, 516–520.

Rouse, R.C., Peacor, D.R. and Freed, R.L. (1988) Pyrophosphate groups in the structure of canaphite, $Ca_2Na_2PO_7.4H_2O$: The first occurrence of a condensed phosphate mineral. *American Mineralogist*, **73**, 168–171.

Rulmont, A., Cahay, R., Liegeois-Duyckaerts, M. and Tarte, P. (1991) Vibrational spectroscopy of phosphate: Some general correlations between structure and spectra. *European Journal of Solid State and Inorganic Chemistry*, **28**, 207–219.

Ryall, W.R. and Segnit, E.R. (1976) Minerals of the oxidized zone of the Dome Rock copper deposit, South Australia. *Australian Mineralogist*, **2**, 5–8.

Segnit, E.R. (1978) Further minerals from the Dome Rock Mine, South Australia. *Australian Mineralogist*, **2**, 73–74.

Shape Software (1997) *ATOMS for Windows and Macintosh V 4.0*. Kingsport, Tennessee, USA.

Sheldrick, G.M. (2008) A short history of *SHELX*. *Acta Crystallographica*, **A64**, 112–122.

Yakubovich, O.V., Massa, W., Liferovich, R.P. and Pakhomovsky, Y.A. (2000) The crystal structure of bakhchisaraitsevite, $[Na_2(H_2O)_2]\{(Mg,Fe)_5(H_2O)_5(PO_4)_4\}$, a new mineral species of hydrothermal origin from the Kovdor phoscorite-carbonatite complex, Russia. *The Canadian Mineralogist*, **38**, 831–838.

Yvon, K., Jeitschko, W. and Parthé, E. (1977) *LAZY PULVERIX*, a computer program, for calculating X-ray and neutron diffraction powder patterns. *Journal of Applied Crystallography*, **10**, 73–74.